ACS APPLIED MATERIALS & INTERFACES

Research Article

www.acsami.org

Chemically Stable and Mechanically Durable Superamphiphobic Aluminum Surface with a Micro/Nanoscale Binary Structure

Shan Peng, Xiaojun Yang, Dong Tian, and Wenli Deng*

College of Materials Science and Engineering, South China University of Technology, Guangzhou 510640, P. R. China

Supporting Information

ABSTRACT: We developed a simple fabrication method to prepare a superamphiphobic aluminum surface. On the basis of a low-energy surface and the combination of micro- and nanoscale roughness, the resultant surface became super-repellent toward a wide range of liquids with surface tensions of 25.3−72.1 mN m^{-1}. The applied approach involved (1) the formation of an irregular microplateau structure on an aluminum surface, (2) the fabrication of a nanoplatelet structure, and (3) fluorination treatment. The chemical stability and mechanical durability of the superamphiphobic surface were evaluated in detail. The results demonstrated that the surface presented an excellent chemical stability toward cool corrosive liquids (HCl/NaOH solutions, 25 °C) and 98% concentrated sulfuric acid, hot liquids (water, HCl/NaOH solutions, 30−100 °C), solvent immersion, high temperature, and a long-term period. More importantly, the surface also exhibited robust mechanical durability and could withstand multiple-fold, finger-touch, intensive scratching by a sharp blade, ultrasonication treatment, boiling treatment in water and coffee, repeated peeling by adhesive tape, and even multiple abrasion tests under 500 g of force without losing superamphiphobicity. The as-prepared superamphiphobic surface was also demonstrated to have excellent corrosion resistance. This work provides a simple, cost-effective, and highly efficient method to fabricate a chemically stable and mechanically robust superamphiphobic aluminum surface, which can find important outdoor applications.

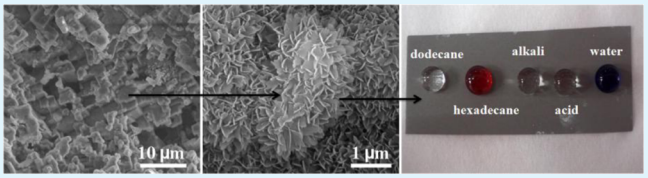

KEYWORDS: *hybrid structures, aluminum, superamphiphobicity, stability, mechanical durability*

1. INTRODUCTION

Many natural surfaces show unique wettability performances, such as plants, including lotus leaves and rice leaves,[1,2] and also animals, including water striders and butterfly wings.[3−5] They are deemed superhydrophobic, characterized by high water contact angles (WCA > 150°) and low sliding angles (SA < 10°). Regarding the broad applications of superhydrophobic surfaces in both academia and industry, researchers have created large numbers of artificial surfaces with superhydrophobicity using a wide variety of methods such as chemical etching,[6,7] colloidal coating,[8,9] anodic oxidation,[10−12] layer-by-layer deposition,[13] hydrothermal synthesis, electrospinning, etc.[14−21]

In contrast to superhydrophobic surfaces, superoleophobic surfaces that achieve contact angles (CAs) above 150° for various oils can be more complicated, but they have a wide range of significant applications in self-cleaning,[22] antifouling,[4] corrosion resistance, and drag reduction.[19,23,24] Researchers have defined the superamphiphobic surfaces as those that are super-repellent to both water and oil. It is demonstrated that such superamphiphobic surfaces are more difficult to fabricate compared to superhydrophobic surfaces. It is well-known that the superhydrophobic effect comes from the combination of a special rough structure and lower surface energy on such surfaces. However, to design superamphiphobic surfaces that resist liquids with lower surface tension, both the surface roughness and surface energy must be strictly controlled. It is generally relatively easy to construct a surface that repels oil liquids with high surface tension but difficult to fabricate a superamphiphobic surface that resists oil fluids that have surface tensions lower than 35 mN m^{-1} (especially one such as dodecane with a surface tension of 25.3 mN m^{-1}).

Although techniques for forming superhydrophobic surfaces are numerous, very few products are launched using real applications mainly because of their poor chemical stability and bad mechanical durability. It is worth noting that many superhydrophobic surfaces lose their superhydrophobic effects quickly when they are exposed to severe and rigorous conditions such as strong acid/alkali solutions, hot liquids, high temperature, a humid environment, oil or solvent contaminants, etc, presenting bad chemical stability. With hot water as an example, most of the previous synthetic superhydrophobic surfaces only show repellence toward cold water under room temperature (around 25 °C); however, they present a remarkably decreased repellency toward hot water (50 °C or higher).[25] Because the water surface tension becomes lower with increasing water temperature, most superhydrophobic surfaces, including natural lotus leaves, are incapable of repelling hot water even when the water temperature becomes a little higher, to say nothing of hot strong acid/alkali

Received: June 1, 2014
Accepted: August 12, 2014
Published: August 12, 2014

 © 2014 American Chemical Society

solutions.[25] Therefore, it is very significant for a superhydrophobic surface that could withstand harsh conditions considering its practical applications. With respect to mechanical robustness, most of the current artificial superhydrophobic surfaces are generally fragile: the rough structures on the surface are easily damaged by impact, finger-touch, or even slight physical rubbing in some cases. When the protuberance morphology required for realization of superhydrophobicity is destroyed by mechanical force, the surface becomes smoother, leading to the loss of the superhydrophobic effect. Furthermore, some superhydrophobic membranes and the hydrophobic layer on such surfaces are easily peeled off and removed, showing weak attachment with the substrate.[26−28] As a result, the poor aging of superhydrophobic surfaces seriously restricts their prospects in industrial applications. It is urgent to improve their mechanical stability for real applications. Recently, great progress has been made in the fabrication of chemically stable and mechanically robust superhydrophobic surfaces.[29−39] Wang et al. fabricated a robust superamphiphobic fabric surface with multiple self-healing ability against both chemical and physical damage by using a two-step surface-coating technique.[38] Wang et al. created robust superhydrophobic fabrics and sponges via the in situ growth of transition-metal oxides and metallic nanocrystals.[37] Xue and Ma reported long-living superhydrophobic colorful surfaces through chemical etching of the fiber surfaces.[36] Wang et al. fabricated a robust superhydrophobic and superoleophilic carbon nanotube/poly(dimethysiloxane)-coated polyurethane sponge for continuous use in oil-spill cleanups.[39] However, these studies mainly focus on the preparation of mechanically robust surfaces based on polymer fabric or sponge substrates. To the best of our knowledge, reports about mechanically durable and chemically stable superhydrophobic metal surfaces are still scarce.[40]

Aluminum and its alloys are important engineering materials. Because of their good ductility, excellent heat and electrical conductivity, and low weight, they find important applications in many modern industrial areas especially in the aerospace, household goods, and automotive industries. Thus, it is very desirable to fabricate a superamphiphobic aluminum surface with superior water- and oil-repellence ability. Up to now, although a variety of methods including electrochemical anodization, phase separation, chemical etching, and sol−gel have been developed to prepare artificial superhydrophobic surfaces based on aluminum substrates,[10,17,18,29,41−44] there are only a few reports involving the realization of a superamphiphobic aluminum surface. Wu et al. designed an unconventional anodized method to fabricate a superoleophobic aluminum surface with low adhesion to diverse oil liquids.[10] Tsujii et al. fabricated a superamphiphobic aluminum surface through an anodic oxidation method.[17] Meng et al. prepared superamphiphobic surfaces on common engineering metals including zinc, aluminum, iron, and nickel via a one-step electrochemical reaction in perfluorocarboxylic acid solutions.[44] However, the above-mentioned methods suffer many problems such as the requirement of a time-consuming process or the limitation to repel certain liquids. Moreover, the chemical stability and mechanical durability of these superamphiphobic surfaces have almost never been investigated and evaluated. In order to achieve outdoor applications, we must pay more attention to the stability of the superamphiphobic surfaces. In our previous work, we have reported a chemically stable and mechanically durable superhydrophobic aluminum surface obtained by an anodized technique. However, this surface is not rough enough to achieve superoleophobicity, which confines its practical applications to some degree.[40]

Here we report a simple, efficient, and time-saving method to fabricate a superamphiphobic aluminum surface with excellent stability against both chemical and physical damage. The raw materials applied in the preparation procedure include aluminum foil with a low purity of 98%, hydrochloric acid, and boiling deionized water, which are all very common and inexpensive. The fabrication process involves two steps: (1) the formation of a microtextured surface through a simple acid etching method; (2) the fabrication of nanoplatelet structures by a boiling water immersion method. The combination of micro- and nanostructures along with the hydrophobic composition could help the surface obtain superamphiphobicity, showing good wetting resistance for various oil liquids with surface tensions ranging from 25.3 to 72.1 mN m^{-1}. The effect of morphology modulation on the surface wettability has also been studied in this work. Moreover, the chemical stability and mechanical durability of the superamphiphobic surface have been examined and evaluated by various methods in detail. The test results have demonstrated that the fabricated superamphiphobic surface is chemically stable toward strong cool liquids (HCl/NaOH solutions, 25 °C) and even 98% concentrated sulfuric acid, hot liquids (water, HCl/NaOH solutions, 30−100 °C), solvent immersion, high temperature, and a long-term period. Furthermore, the surface also shows excellent mechanical durability and can withstand multiple-fold, finger-touch, intensive scratching by a sharp blade, repeated peeling by adhesive tape, ultrasonication treatment, boiling treatments in water and coffee, and even abrasion tests under 500 g of force without losing superamphiphobicity. The corrosion resistance to diverse solutions of the as-prepared superamphiphobic surface was also examined.

2. EXPERIMENTAL SECTION

2.1. Specimen Preparation. Aluminum plates (thickness, 0.25 mm; composition, Al of 98%, Si of 0.3%, and O of 1.7%) and hydrochloric acid (HCl) were obtained from Guangzhou QianHui Materials Co., Guangzhou, P.R. China; 1*H*,1*H*,2*H*,2*H*-perfluorodecyltriethoxysilane (PDES) was purchased from Alfa Aesar Co., Tianjin, P.R. China. All other chemicals were of analytical grade and were used as received.

In a typical procedure, the aluminum plates were cut into small pieces and ultrasonically cleaned with acetone, ethanol, and deionized water in sequence to get rid of grease and purities. The cleaned aluminum plates were next etched in a 2.5 M HCl solution for 8 min at room temperature to obtain a microstructured surface. After the etching process, the samples were rinsed with deionized water and dried at 120 °C for 10 min. The microstructured aluminum plates were next immersed in boiling deionized water for 15 min and subsequently dried with nitrogen. Finally, the as-prepared samples were dipped in a 1.0 wt % ethanol solution of PDES for 30 min and then heated at 100 °C for 1 h (the preparation time of the superamphiphobic surface here was demonstrated to be less than 1 h).

2.2. Specimen Characterization. The surface structures and chemical compositions of the as-prepared samples were determined by field-emission scanning electron microscopy (FESEM; Nova Nano-SEM 430) via energy-dispersive spectroscopy (EDS; X-Max 20, Oxford Instruments, Oxford, England). The water contact angles (WCAs) and sliding angles (SAs) were determined using an OCA35 (Data Physics, Wetzhausen, Germany) equipped with a video camera and a tilting stage. SAs were measured by slowly tilting the sample stage until the water droplet started moving. The static WCA and SA values were the averages of five measurements obtained at diverse positions using 3−5 μL water droplets. The photography was done

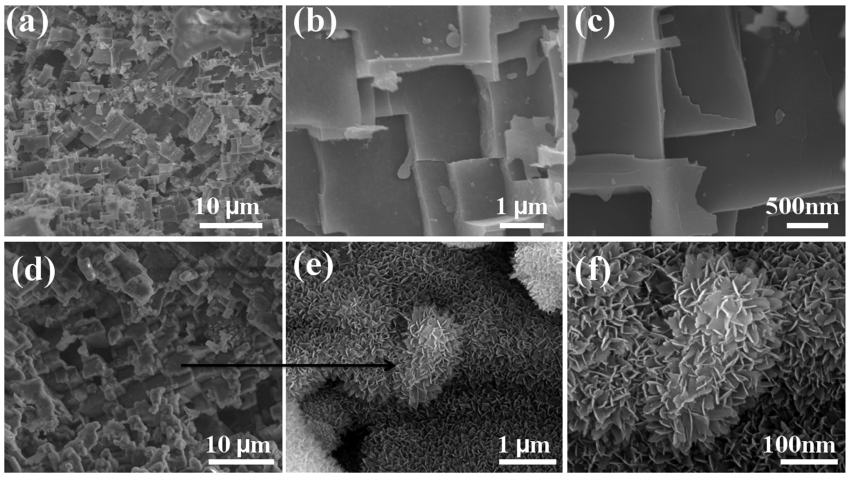

Figure 1. (a–c) Low- and high-magnification FESEM images of the aluminum surface after etching in a HCl solution for 8 min (MS-surface). (d–f) Low- and high-magnification FESEM images of the surface after subsequent treatment by immersion in boiling water for 15 min (MNS-surface).

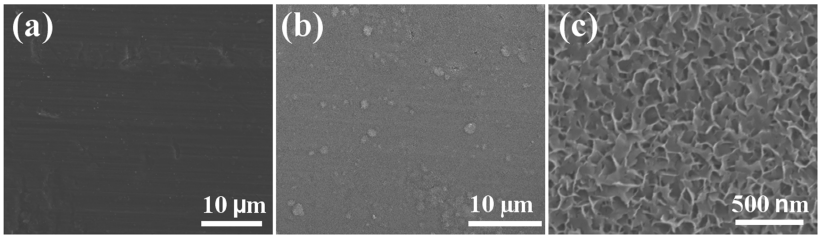

Figure 2. (a) FESEM image of the flat aluminum surface. (b and c) Low- and high-magnification FESEM images of the aluminum surface after immersion in boiling water for 15 min.

using a digital camera (Canon). The electrochemical measurements were conducted in 3.5 wt % aqueous solutions of NaCl and Na_2SO_4 at room temperature using an electrochemical workstation (IM6ex, Zahner, Germany). The electrochemical corrosion tests were carried out using a three-electrode configuration with platinum as the counter electrode, saturated calomel as the reference electrode, and samples with an exposed area of 1 cm^2 as the working electrode (the working electrode is in a vertical position during the tests). The potentiodynamic polarization was tested at a scanning rate of 5 mV s^{-1}. The Tafel regions were obtained from the range of E_{ocp} (open-circuit potential) ± 50 mV. Every potentiodynamic polarization curve result was performed a minimum of four times.

3. RESULTS AND DISCUSSION

In order to better understand the significance of the combination of micro- and nanostructures on the preparation of a superamphiphobic aluminum surface, we compare the morphology and wettability of the micro/nanostructured aluminum surface (MNS-surface) with those of a micro-structured aluminum surface (MS-surface) and a nano-structured aluminum surface (NS-surface). Parts a–c of Figure 1 present top-view FESEM images of the MS-surface obtained by etching in a HCl solution for 8 min. It can be clearly observed that a fractal structure with numerous facets was formed (Figure 1a). The entire aluminum surface became rough and composed of large amounts of irregular "protrusions" immediately after acid treatment. The high-magnification FESEM images demonstrated that the MS-surface composed of irregular microprotrusions, which appeared like building blocks, consisted of rectangular-shaped plateaus with the size of a few microns (Figure 1b,c). The concept result in these types of microstructures by acid treatment was established almost a half-century ago. A large number of dislocation defects that own relatively higher energy exist in common crystalline metals. These dislocation sites are prone to attack by chemical etchants and would dissolve first. Selective corrosion effects lead to large amounts of micropits on the surface to form a kind of labyrinthine morphology.[7,30] It is worth noting that those plateau surfaces in this case are smooth. However, with the subsequent treatment of immersion in boiling water for 15 min, a huge morphology change can be seen. As shown in Figure 1d, the surface becomes rougher after treatment with boiling water. The plateaus are not smooth anymore, and a large number of nanoplatelets are produced on the plateaus in this case (Figure 1e). The nanoplatelets are 20–40 nm in size and are distributed throughout the whole surface. It seems like those nanoplatelet structures tend to aggregate with each other to form a kind of flowerlike morphology (Figure 1f). The cross-sectional FESEM image of the MNS-surface indicates that the MNS-surface presents the expected reentrant surface structure, which is the key parameter in obtaining superoleophobicity (Figure S1 in the Supporting Information, SI). During this boiling water immersion treatment, a chemical reaction between the initial native oxide layer on the aluminum surface and water happens at the primary stage, resulting in the formation of $Al_2O_3{\cdot}xH_2O$. Moreover, some generated $Al_2O_3{\cdot}xH_2O$ can further react with water to form crystalline boehmite, while partial boehmite would dissolve in the boiling water.[45−47] The formation of large-scale nanoplatelet morphology may be ascribed to the physical attack of dihydrogen and air bubbles at the boiling water/aluminum interface. Thus, when the above-mentioned preparation steps (acid etching followed by boiling water immersion) are combined, the MNS-surface is obtained. This hybrid surface structure with a finely constructed micro/

nanosurface, together with the presence of the PDES layer, endows the finished surface with superamphiphobicity.

To obtain the NS-surface, we performed a comparative experiment by immersing a flat aluminum plate into boiling water for 15 min, and its resultant surface structures are shown in Figure 2. The aluminum plate was originally flat (Figure 2a); however, the surface was quickly covered with a large number of distorted nanoflakes with thicknesses of 20−40 nm after the boiling water immersion treatment (Figure 2b,c). It is obvious that only the pure nanoflake structures are produced in this case.

Parts a−d of Figure 3 show the EDS spectra of the untreated aluminum plate, unmodified MS-surface, and unmodified and

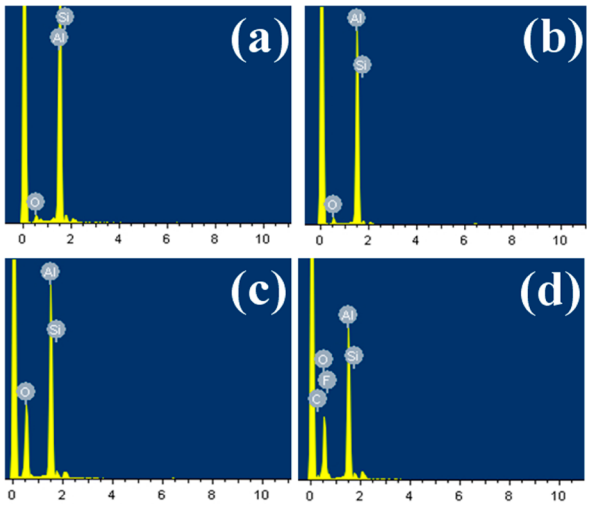

Figure 3. EDS spectra of the (a) flat aluminum surface, (b) MS-surface, and (c) MNS-surface before and (d) after PDES modification.

PDES-modified MNS-surfaces. When the results of Figure 3a,b are compared, we find that no additional element occurred after the acid etching treatment. However, the ratio of the O element increased greatly after the boiling water treatment, indicating the formation of $Al_2O_3{\cdot}xH_2O$. Compared to the composition of Figure 3c, the superamphiphobic MNS-surface consisted of elemental Al, O, Si, F, and C (Figure 3d), indicating that the PDES film was self-assembled on the surface successfully. Owing to the existence of the $-CF_3$ and $-CF_2$ groups (6.7 and 18 mJ m^{-2} surface energy, respectively), PDES has a very low surface free energy and can effectively decrease the free energy of the as-prepared surface. A previous report also confirmed that the silane molecule would be strongly anchored to the aluminum substrate by reaction of the hydrolysis silane species with the surface functional groups (Al−OH) of the aluminum surface to form a self-assembled monolayer with low surface energy.[48] The formation scheme of the self-assembly of the PDES film on the MNS-surface is shown in Figure S2 in the SI.[49] First, the silicon ethyoxyl ($Si-OCHH_2CH_3$) groups react with water to produce silanols (Si−OH), which act as reactive groups at the end of the molecule. These silanols subsequently combined with the OH groups to form a self-assembled film. Meanwhile, the surface can also induce vertical polymerization to form a grafted polysiloxane.[11]

Figure 4 shows the surface wettability of diverse PDES-modified surfaces by using different liquid droplets. A close inspection of the data reveals that all (MNS, MS, and NS) surfaces display excellent superhydrophobicity but various

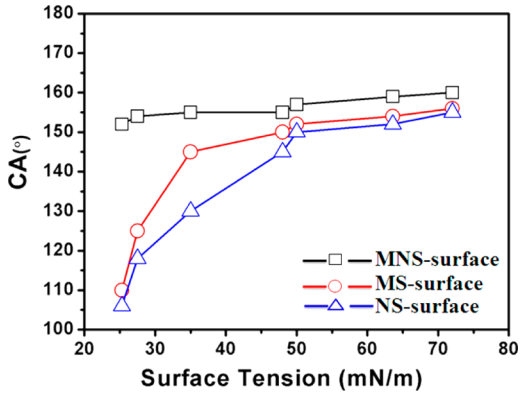

Figure 4. Relationship between the CAs and liquid droplets with diverse surface tension measured on various fabricated surfaces. The surface tensions are in the range of 25.3−72.1 mN m^{-1}. The error limit of the CA value here is ∼1°.

oleophobicity after the fluorination treatment. The CA value on the MNS-surface for each kind of liquids is higher than those of the MS- and NS-surfaces, indicating that the MNS-surface obtains improved oleophobicity compared to the MS/NS-surface. Previous reports have demonstrated that superoleophobicity can be achieved by introducing special features such as a reentrant curvature structure and an overhanging geometry.[50,51] Such structures are essential to form a composite solid−liquid−air interface with oil liquids and can effectively prevent liquids from penetrating into the cavities. In our studies, the pure rectangular structure of the MS-surface and the single nanoplatelet morphology of the NS-surface are not rough enough to obtain superoleophobicity for the hexadecane droplet, while the MNS-surface possesses the ability to achieve a hexadecane CA of 154° and even a dodecane CA of 152°, demonstrating that the combination of both micro- and nanoscale surface features creates the particular geometry required for repellence toward oil liquids with lower surface energy.

The optical top-view and side-view images of the different droplets on the MNS-surface are highlighted in parts a and b of Figure 5, respectively. Considering that hexadecane and dodecane are oil liquids with very low surface tension and they are also widely and normally used solvents in our real life and industry (Table S1 in the SI), we choose them as typical oil

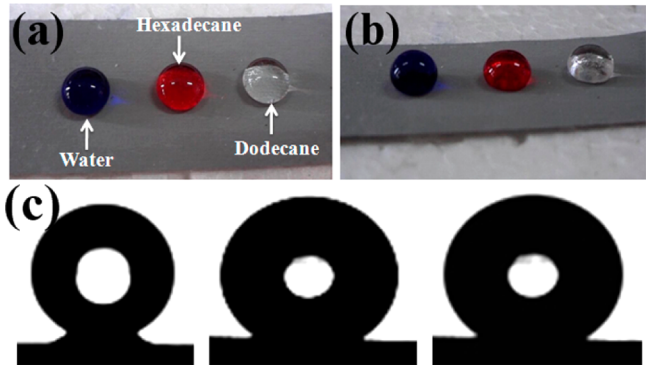

Figure 5. Top-view (a) and side-view (b) optical images of different liquid droplets on the MNS-surface. The droplets are water, hexadecane, and dodecane in sequence. (c) CA shapes of the three liquid droplets. The CAs are 160°, 154°, and 152°, respectively. The error limit of the CA value here is ∼1°.

droplets to evaluate the superoleophobicity of our MNS-surface. It can be seen that all water, hexadecane, and dodecane droplets exhibit typical spherical shapes on the surface. The CAs on the MNS-surface for the three liquids are 160°, 154°, and 152°, respectively, demonstrating the excellent superhydrophobicity and superoleophobicity of the surface. Comparisons of the SAs for various liquids on diverse fabricated surfaces are shown in Table 1, which further confirms that only the surface structure on the MNS-surface can achieve superoleophobicity for hexadecane and dodecane with the lower surface tension.

Table 1. Comparisons of the SAs (deg) of Diverse Liquids on Various Surfaces[a]

liquid	surface tension (mN m^{-1}) (20 °C)	MNS-surface	MS-surface	NS-surface
water	72	0	1	0
glycerol	63	2	5	5
CH_2I_2	50	2	10	8
ethylene glycol	48	3	20	13
rapeseed oil	35	10	38	N.S.
hexadecane	27.5	15	N.S.	N.S.
dodecane	25.3	25	N.S.	N.S.

[a]The error limit of the SA value is ~0.5°. N.S.: no sliding.

Furthermore, we also investigated the effects of the boiling water immersion time on the surface morphology and wettability. Figure 6 shows the FESEM images of the resultant

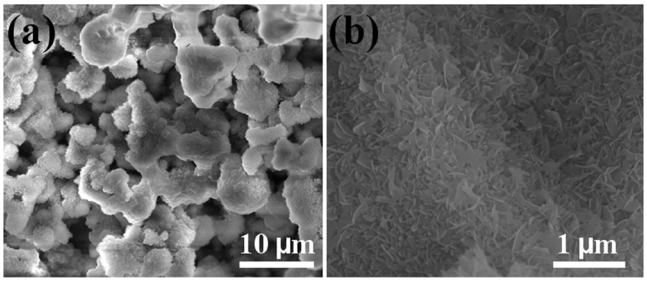

Figure 6. (a) Low- and (b) high-magnification FESEM images showing the surface structure of the aluminum surface obtained by first etching in a HCl solution for 8 min, followed by immersion in boiling water for 1 h.

aluminum surface fabricated by controlling the immersion time in boiling water. When the immersion time was prolonged to 1 h, it was found that the surface macroscopic overhang structure was broken and the nanoplatelet morphology became flat.

The corresponding CAs for various liquids on the diverse surfaces are presented in Figure 7. It can be observed that the CAs of the 1 h immersion surface are lower than those of the MNS-surface. The roughness of the 1 h immersion surface is demonstrated to be insufficient to obtain superoleophobicity to repel oil liquids such as hexadecane or dodecane. These results further confirm that the dual structure with sufficient roughness is very crucial to achieving superoleophobicity toward oil droplets with lower surface tension.

We further studied the surface morphology of aluminum fabricated in hot water with different temperatures, and the high-magnification FESEM images are shown in Figure S3 in the SI. This confirmed that nanoplatelet structures could also

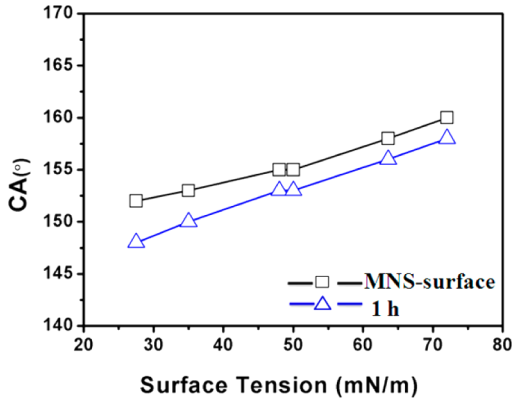

Figure 7. CAs as a function of the liquid surface tension measured on diverse as-prepared surfaces. The error limit of the CA value here is ~1°.

be formed in 60 and 80 °C hot water conditions. However, because of the moderate reaction under lower water temperature, the nanoplatelet morphology formed was sparsely distributed on the surface and the size of the nanoplatelet was smaller than that of the surface reacted in boiling water (Figure 1f). The surface fabricated under 60 or 80 °C was also demonstrated to show worse superoleophobicity toward low-surface-tension liquids (hexadecane and dodecane), which further indicated the important role of surface roughness in obtaining superoleophobicity.

For outdoor applications, it is of major significance to evaluate the durability and robustness of a superamphiphobic surface under different severe conditions. In this study, we have conducted a series of approaches to test the chemical stability and mechanical durability of the resultant MNS-surface. The superamphiphobic MNS-surface has a superior resistance toward 98% concentrated sulfuric acid. It could repel 98% sulfuric acid droplets quickly without any trace (Figure S4 in the SI). On the contrary, when the 98% concentrated sulfuric acid rolled off the superhydrophobic MS-surface, parts of the acid trace were left on the surface (Figure S4 in the SI). This phenomenon demonstrated that the nonwetting property of the MS-surface was worse than that of the MNS-surface. The 98% sulfuric acid droplets dropped on the MNS-surface would maintain spherelike shape for at least 30 min. After the acid was removed and the surface was cleaned, the surface was still superamphiphobic (Figure S5 in the SI). It seems that the concentrated sulfuric acid almost does not create effects on the MNS-surface. As shown in Figure 8a, the WCAs remain above 150° and the SAs remain below 10° for liquid solutions with diverse pH values on the MNS-surface, demonstrating that the surface is highly stable against chemical corrosion. Because of the versatile and complex conditions in our real life, the ability of the superhydrophobic surface to resist hot liquids is a very vital consideration in practical applications. However, in most previous reports related to superhydrophobic surfaces, researchers tend to use cool water (about 25 °C) to evaluate the wettability and adhesion properties of these superhydrophobic surfaces. Few papers involving the repellent ability of the superhydrophobic surfaces to hot liquids have been reported.[25,40] Thus, in this paper, we examine this kind of performance of our as-prepared MNS-surface by using several kinds of liquids including hot water and hot HCl (pH = 1)/NaOH (pH = 14) solutions with the temperature ranging from 30 to 100 °C. To our surprise, the superamphiphobic MNS-

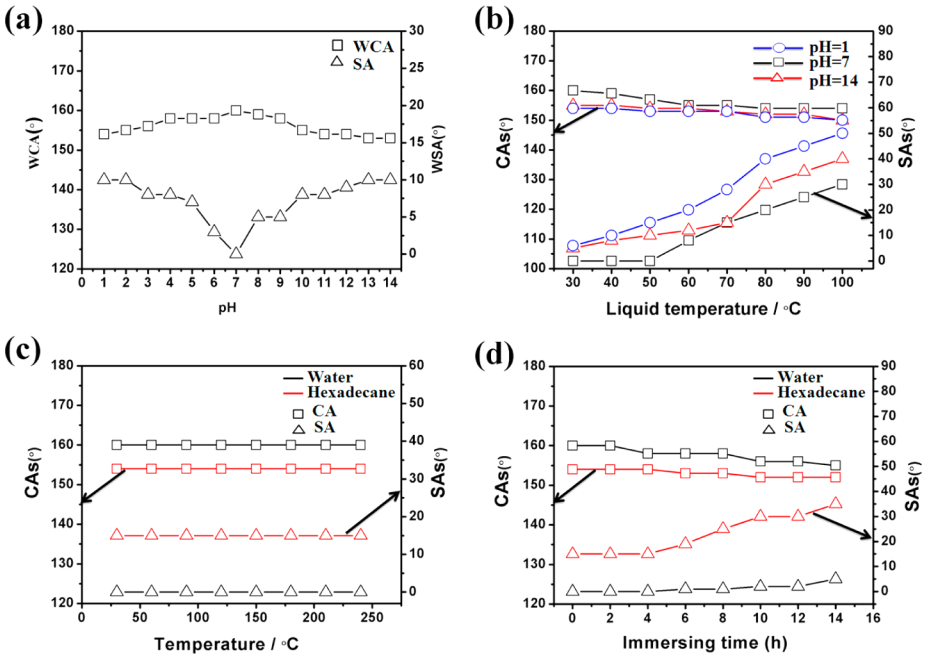

Figure 8. Variations of the liquid repellence of the MNS-surface under various harsh conditions. (a) Relationship between the pH and WCA and SA values of the MNS-surface. (b) Variations of the CAs and SAs on the MNS-surface after the addition of hot liquid droplets with diverse pH (strong HCl solution with a pH of 1, water with a pH of 7, and a strong NaOH solution with a pH of 14) under the liquid-temperature scope of 30−100 °C. (c) CAs and SAs of water and hexadecane on the MNS-surface under diverse surface temperatures ranging from 30 to 250 °C. (d) CAs and SAs of water and hexadecane on the MNS-surface after immersion in a solvent solution for diverse amounts of time. The error limits of the CA and SA values here are ∼1° and ∼0.5°, respectively.

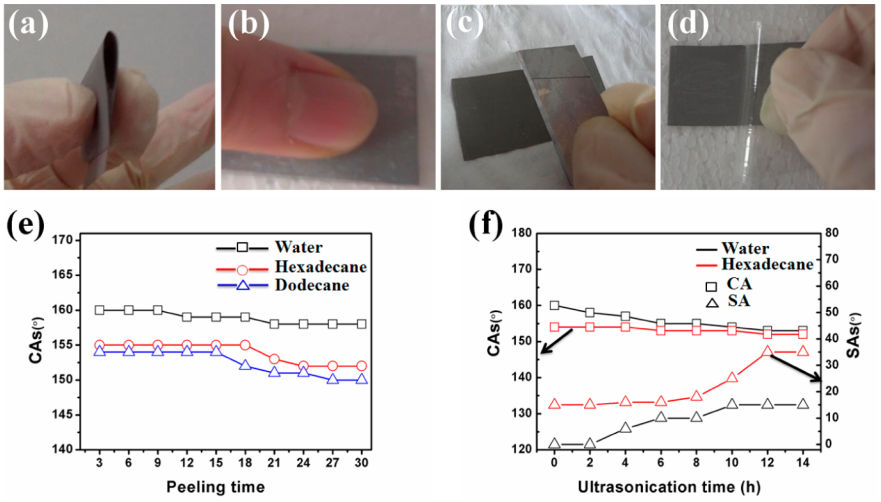

Figure 9. Qualitative tests of mechanical durability through (a) multiple folds, (b) finger pressing, (c) scratching with a sharp blade, and (d) multiple peelings with adhesive tape. (e) CAs of various droplets measured with respect to the peeling times on the MNS-surface. (f) CAs of water and hexadecane on the MNS-surface measured with respect to the ultrasonication time in a solvent. The error limits of the CA and SA values here are ∼1° and ∼0.5°, respectively.

surface also has excellent resistance toward hot water, even hot HCl or NaOH solutions with temperatures as high as 100 °C (Figure S6 in the SI). As can be seen from the testing results of Figure 8b, the MNS-surface can repel cool liquids (around 30 °C) very quickly and achieve high WCAs and low SAs in this case. With increasing liquid temperature, the CAs decrease slightly while the SAs show an increasing trend. However, the CAs can also be maintained above 150° toward hot HCl/NaOH solution droplets even at 100 °C. The SA values become larger with increasing temperature, which demonstrates that the surface becomes a little sticky toward the liquids at higher temperature. Even so, the relatively small changes about the CA and SA values further demonstrate that our obtained MNS-surface is highly stable against chemical corrosion and liquids under high temperature, which is scarcely realized in many reported superhydrophobic surfaces. It also should be noted that the superamphiphobic surface shows especially superior stability against high surface temperature. As indicated in Figure 8c, it seems that the surface temperatures almost do not create any changes of the WCA and SA values for water and hexadecane. The superhydrophobicity and superoleophobicity remain the same even when the temperature is as high as 250

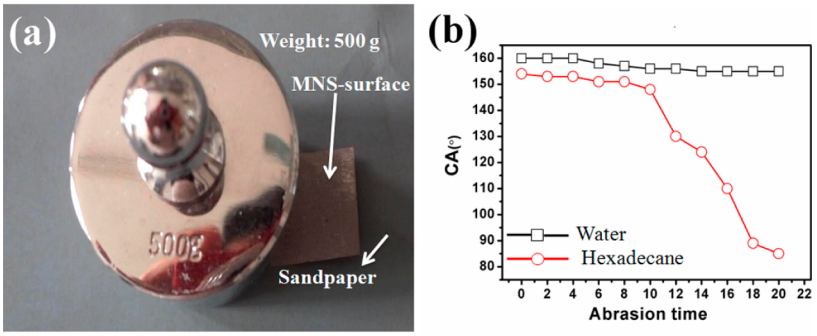

Figure 10. (a) Abrasion treatment of the MNS-surface with sandpaper. (b) CAs of water and hexadecane measured with respect to the abrasion times on the MNS-surface. The error limit of the CA value here is ~1°.

°C, further confirming that the surface possesses superior stability when exposed under a drastic temperature environment. When the superamphiphobic surface is exposed under room conditions for 6 months, it shows no changes in water and hexadecane, indicating its long-term stability (Figure S7 in the SI). The MNS-surface can also withstand exposure to other serious conditions. As shown in Figure 8d, the CAs for water and hexadecane are still above 150° even after the MNS-surface is soaked in organic solvents (ethanol) for 24 h.

One of the greatest problems facing the widespread application of superhydrophobic surfaces is usually their mechanical susceptibility to mechanical press or abrasion. In most cases, even slightly abrasive forces or simple rubbing can easily damage or destroy the fine-scale surface structure, which is indispensable for realizing a superhydrophobic effect.[52] For example, when a synthetic superhydrophobic surface is touched by a bare hand, the affected area region of the surface would be contaminated by salt and oil, which would lead to increasing surface energy and finally result in an immediate loss of superhydrophobicity. The robustness and mechanical performance of our resultant surface were evaluated through a series of test methods. First, the MNS-surface was assessed qualitatively by simple multiple-fold tests, pressing with a bare hand, and scratching with a sharp blade (Figure 9a–c). It was found that the superhydrophobicity and superoleophobicity of the MNS-surface remained unchanged after the multiple-folding and bare finger-touching treatments (Figure S8 in the SI). Even a finger that was full of wet salt and oil (our finger was purposely dipped in a mixed solution of NaCl and glycerol) did not induce any effects on the superamphiphobicity of the as-prepared MNS-surface (video S1 in the SI), indicating its excellent mechanical stability compared with some superhydrophobic surfaces treated in a similar way. Besides the folding and finger-touching treatments, intensive scratching with a sharp blade could remove the fluorine layers and break the delicate structure of the MNS-surface but creates almost no influence on its water-rolling behavior (Figure S8 and video S2 in the SI). In order to quantize the scratching force applied on the surface, we designed a handmade device to measure it (Figure S9 in the SI). Then we next investigated the morphology and corresponding wettability variations of the superamphiphobic MNS-surface after the scratch treatment for one time under various weights. The topography changes of the MNS-surface after scratching tests under 200, 400, 500, and 700 g of force are shown in Figure S8 in the SI. We could observe that a slight scratching force of 200 g did not create serious effects on the special overhang structure of the MNS-surface (Figure S8a in the SI). However, with increasing force, the surface structure was damaged more and more severely, and the surface almost became flat under a heavy force of 700 g (Figure S8b–d in the SI). The CA variations for water and hexadecane under diverse weights are presented in Table S2. As can be seen, the CA values for water are still maintained above 150° even after the scratching test under a force of 700 g, while the CAs for hexadecane remained above 150° when the force was less than 300 g. However, the repellence toward hexadecane was lost when the applied force was more than 500 g. We then take a careful observation of the remaining surface structure after the scratching test under a force of 500 g (Figure S8e,f in the SI). Considering the special surface structure of the MNS-surface, it is easy to observe that huge height differences exist on the whole surface. When the higher position on the surface was damaged by the mechanical force, the hierarchical structure positioned at the lower place on the surface could still be maintained. Furthermore, from the high-magnification images (Figure S8e,f in the SI), it could be seen that the damaged MNS-surface did not become smooth totally and many chunks with nanoplatelet structures (all of these nanoplatelets combined with the PDES layer) covered the surface disorderly. From the above-mentioned reasons, we can explain the main reasons for preservation of the superamphiphobicity of the MNS-surface after the scratching test. To further investigate the robustness of the superamphiphobic MNS-surface, we exposed the surface to more rigorous conditions such as multiple-peeling tests by adhesive tape. As shown in Figure 9d, the adhesive tape was pressed against the superamphiphobic MNS-surface intimately and then peeled off immediately. Figure 9e shows the relationship between the CAs and peeling times. It confirmed that the CAs for water and hexadecane could still remain above 150° even after repeated peeling tests up to 30 times. When measuring the SA value, we found that it increased with more peeling attempts; however, it could still achieve a WSA of 35° after the peeling test was repeated 30 times. These results demonstrated that the as-prepared superamphiphobic surface layer had a good adhesive attachment with the substrate and retained its superamphiphobicity after the adhesive tests, indicating excellently mechanical durability of the MNS-surface.

The MNS-surface also shows excellent stability against boiling treatments in water and coffee. After being treated in boiling water for 1 h, the surface still maintains its liquid-repellence performance. Moreover, the surface also has a fascinating self-cleaning ability. After boiling in coffee for 1 h, followed by cleaning with water and drying under room temperature, the surface was not stained and showed no change in superamphiphobicity (Figure S11 in the SI). Such excellent

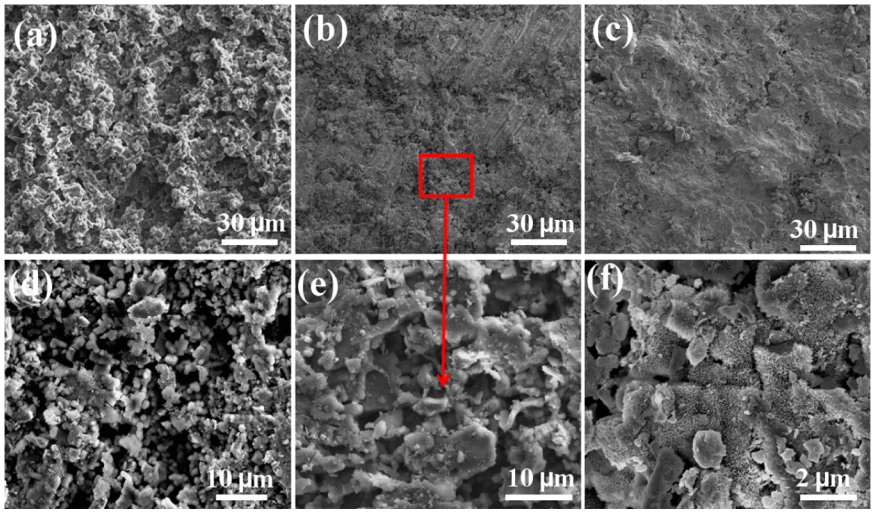

Figure 11. FESEM images of the MNS-surface after the abrasion treatment for various times: (a) 3; (b) 10; (c) 25. (d) High-magnification image of the red region in part b. (e and f) Further magnified FESEM images of part d.

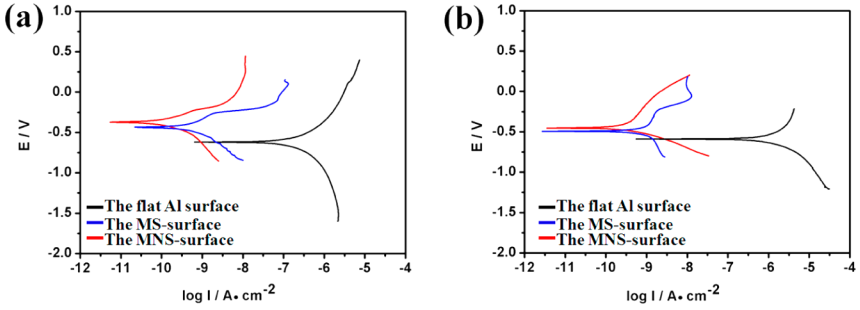

Figure 12. Potentiodynamic polarization curves of the flat aluminum and MS- and MNS-surfaces in different corrosive solutions: (a) 3.5 wt % NaCl aqueous solution; (b) 3.5 wt % Na_2SO_4 aqueous solution.

nonwetting and heat-resistance properties of the superamphiphobic MNS-surface were very effective for self-cleaning of contaminants under harsh conditions. The structure of the MNS-surface after boiling water treatments for 1 h is presented in Figure S12 in the SI. As can be seen, the whole overhang structure was still maintained, and the nanoplatelet structures almost showed no change after the treatments.

The mechanical robustness of the surface was further studied by more rigorous abrasion tests, which were carried out back and forth with sandpaper at a rate of 5 cm s^{-1} under 500 g of force for various repeated cycles (Figure 10a). The changes in static CAs for water and hexadecane droplets on a superamphiphobic MNS-surface with increasing abrasion cycles are presented in Figure 10b. As can be seen from this figure, although the WCA decreased slightly during the scope, it still maintained 155° even after treatment by abrasion cycles as high as 20 times under a 500 g of force. Meanwhile, although the hexadecane CA decreased to 85° after a 20 times abrasion test, it remained above 150° over the first 10 cycles. These phenomena further demonstrated that our as-prepared surface possessed a superior mechanical stability even under the abrasion tests with 500 g of force up to 20 times, which was even scarcely realized in many other superhydrophobic metal surfaces. The pictures and videos of the liquid droplets on the MNS-surface after severe mechanical damage further convictively confirmed the above-mentioned conclusions (Figure S13 and videos S3 and S4 in the SI). Figure 11 showed the surface structure of the MNS-surface after being abraded under 500 g of force 5, 10, and 25 times, respectively. The first five abrasion times induced mild destruction on the surface feature of the MNS-surface, and the whole "overhang" morphology still remained (Figure 11a). With increasing abrasion times, the surface became smoother, and finally the delicate micro-nanostructure was mostly destroyed (Figure 11c). With careful observation of the high-magnification SEM images of Figure 11b, it was found that, although some regions positioned at the top of the surface were damaged by mechanical force, the hierarchical structure at the lower position of the surface was still maintained (Figure 11d–f). More importantly, some chunks with the nanoplatelet flowerlike structure induced from the abrasion treatment were disorderly distributed on the surface. These topographies combined with the fluorine material layer could also contribute the reserve of superamphiphobicity of the MNS-surface after the abrasion treatment.

In order to investigate the fascinating stability of the resultant MNS-surface, we further studied the corrosion resistance of the superamphiphobic MNS-surface. Typically, a lower corrosion current density or a higher corrosion potential corresponds to a better corrosion resistance. The potentiodynamic polarization curves of the flat aluminum, superhydrophobic MS-surface, and superamphiphobic MNS-surface in the diverse aqueous corrosion solutions are obtained using the Tafel extrapolation method and are presented in Figure 12. A careful inspection of the data reveals that the corrosion potentials (E_{corr}) of the superamphiphobic MNS-surface and MS-surface are more

positive than that of the flat aluminum surface, whether in a 3.5 wt % aqueous solution of NaCl or Na_2SO_4, suggesting good protection for the aluminum substrate by the superamphiphobic or superhydrophobic layer. It can also be clearly observed that the corrosion current densities (I_{corr}) of the MS-surface and MNS-surface are much lower than that of the flat aluminum surface in the two corrosive solutions. These results indicated that both the superhydrophobic layer on the MS-surface and superamphiphobic layer on the MNS-surface greatly improved the corrosion resistance of the resultant aluminum substrate in comparison with the flat aluminum surface. However, the superamphiphobic MNS-surface achieves the highest E_{corr} and lowest I_{corr} values, showing the most superior corrosion resistance ability. These results prove that the surface roughness plays an important role in obtaining superior corrosion resistance of the MNS-surface. Besides the surface roughness, we believe that the surface composition also has a vital role in achieving excellent corrosion resistance. In order to figure out the influence of the PDES layer on the corrosion resistance of the superamphiphobic MNS-surface, we used stearic acid (STA) to modify the MNS-surface (the MNS-surface was dipped into a 5 mM ethanol solution of STA for 2 h) and further tested its potentiodynamic polarization curves in 3.5 wt % NaCl aqueous solutions. We also measured the corrosion resistance of the unmodified MNS-surface in the same conditions, and the potentiodynamic polarization curves of these diverse samples are summarized in Figure S14 in the SI. We can observe that the unmodified MNS-surface only slightly improves the corrosion resistance. Although the STA-modified MNS-surface also shows improved corrosion resistance, its ability is still weaker than that of the PDES-modified MNS-surface. These results sufficiently prove that the PDES layer has a very significant role in acquiring excellent corrosion resistance. Because PDES has very low surface energy, it can effectively and greatly decrease the surface energy. The PDES layer, when combined with the sufficient roughness of the MNS-surface, can protect the aluminum substrate from corrosive solutions.

4. CONCLUSIONS

We have developed a cost-effective, easy-to-implement, and time-saving method to fabricate a superamphiphobic aluminum surface. When the simple chemical etching and boiling water immersion processes were combined, dual structures, including microplateaus and nanoplatelets, were successfully built on the surface and were also demonstrated to play a significant role in realizing superamphiphobicity. The resultant surface could achieve super-repellence toward a wide range of liquids with a surface tension range of 25.3−72.1 mN m^{-1}. The fabricated MNS-surface exhibits excellent chemical stability and fascinating mechanical durability after numerous tests. It is found that the surface can maintain its chemical stability when exposed to strong acid/alkali solutions (even 98% concentrated sulfuric acid), hot water/acid/alkali solutions (the liquid temperature could even reach as high as 100 °C), solvent immersion, high temperature, and a long-term period. With respect to the mechanical durability, the results demonstrate that the surface presents an amazing resistance toward multiple-fold, finger-touch (even when the finger was full of oil and salt), intensive scratching with a sharp blade, repeated peeling by adhesive tape, ultrasonication treatment, boiling treatments, and even multiple abrasion tests under 500 g of force without losing superamphiphobicity. The current method has proven to be suitable for large-scale industrial fabrication of chemically stable and mechanically robust superamphiphobic surfaces, which can realize a true potential for many industrial applications.

■ ASSOCIATED CONTENT

Supporting Information

Additional figures and tables, video S1 showing the finger-contact process of the MNS surface, video S2 showing the scratching treatment on the MNS surface with a sharp blade, video S3 showing the multiple peeling process of the MNS surface, and video S4 showing the abrasion process of the MNS surface. This material is available free of charge via the Internet at http://pubs.acs.org.

■ AUTHOR INFORMATION

Corresponding Author

*Phone: (+86)020-22236708. E-mail: wldeng@scut.edu.cn.

Notes

The authors declare no competing financial interest.

■ ACKNOWLEDGMENTS

Financial support from the National Natural Science Foundation of China (Grants 21103053, 91023002, and 51073059), the National Program on Key Basic Research Project (Grants 2012CB932900 and 2009CB930604), and the Cooperation Project in Industry, Education and Research of Guangdong Province and Ministry of Education of China (Grant 2011B090400376) is gratefully acknowledged. Thanks also go to Professor Kang Zhixin for his experimental help.

■ REFERENCES

(1) Barthlott, W.; Neinhuis, C. Purity of the Sacred Lotus, or Escape from Contamination in Biological Surfaces. *Planta* **1997**, *202*, 1−8.
(2) Herminghaus, S. Roughness-Induced Non-Wetting. *Europhys. Lett.* **2000**, *52*, 165.
(3) Gao, X.; Jiang, L. Biophysics: Water-Repellent Legs of Water Striders. *Nature* **2004**, *432*, 36−36.
(4) Genzer, J.; Efimenko, K. Recent Developments in Superhydrophobic Surfaces and Their Relevance to Marine Fouling: a Review. *Biofouling* **2006**, *22*, 339−360.
(5) Parker, A. R.; Lawrence, C. R. Water Capture by a Desert Beetle. *Nature* **2001**, *414*, 33−34.
(6) Saleema, N.; Sarkar, D.; Gallant, D.; Paynter, R.; Chen, X.-G. Chemical Nature of Superhydrophobic Aluminum Alloy Surfaces Produced via a One-Step Process Using Fluoroalkylsilane in a Base Medium. *ACS Appl. Mater. Interfaces* **2011**, *3*, 4775−4781.
(7) Qian, B.; Shen, Z. Fabrication of Superhydrophobic Surfaces by Dislocation-Selective Chemical Eetching on Aluminum, Copper, and Zinc Substrates. *Langmuir* **2005**, *21*, 9007−9009.
(8) Li, X.; Shen, J. A Facile Two-Step Dipping Process Based on Two Silica Systems for a Superhydrophobic Surface. *Chem. Commun.* **2011**, *47*, 10761−10763.
(9) Wang, N.; Xiong, D. Influence of Trimethylethoxysilane on the Wetting Behavior, Humidity Resistance and Transparency of Tetraethylorthosilicate Based Films. *Appl. Surf. Sci.* **2014**, *292*, 68−73.
(10) Wu, W.; Wang, X.; Wang, D.; Chen, M.; Zhou, F.; Liu, W.; Xue, Q. Alumina Nanowire Forests via Unconventional Anodization and Super-repellency Plus Low Adhesion to Diverse Liquids. *Chem. Commun.* **2009**, 1043−1045.
(11) Xu, W.; Song, J.; Sun, J.; Lu, Y.; Yu, Z. Rapid Fabrication of Large-area, Corrosion-Resistant Superhydrophobic Mg Alloy Surfaces. *ACS Appl. Mater. Interfaces* **2011**, *3*, 4404−4414.
(12) Peng, S.; Tian, D.; Miao, X.; Yang, X.; Deng, W. Designing Robust Alumina Nanowires-on-Nanopores Structures: Superhydro-

phobic Surfaces with Slippery or Sticky Water Adhesion. *J. Colloid Interface Sci.* **2013**, *409*, 18−24.
(13) Zhai, L.; Cebeci, F. Ç.; Cohen, R. E.; Rubner, M. F. Stable Superhydrophobic Coatings from Polyelectrolyte Multilayers. *Nano Lett.* **2004**, *4*, 1349−1353.
(14) Lim, H. S.; Kwak, D.; Lee, D. Y.; Lee, S. G.; Cho, K. UV-Driven Reversible Switching of a Roselike Vanadium Oxide Film between Superhydrophobicity and Superhydrophilicity. *J. Am. Chem. Soc.* **2007**, *129*, 4128−4129.
(15) Ganesh, V. A.; Nair, A. S.; Raut, H. K.; Tan, T. T. Y.; He, C.; Ramakrishna, S.; Xu, J. Superhydrophobic Fluorinated POSS−PVDF−HFP Nanocomposite Coating on Glass by Electrospinning. *J. Mater. Chem.* **2012**, *22*, 18479−18485.
(16) Lin, J.; Cai, Y.; Wang, X.; Ding, B.; Yu, J.; Wang, M. Fabrication of Biomimetic Superhydrophobic Surfaces Inspired by Lotus Leaf and Silver Ragwort Leaf. *Nanoscale* **2011**, *3*, 1258−1262.
(17) Tsujii, K.; Yamamoto, T.; Onda, T.; Shibuichi, S. Super Oil-Repellent Surfaces. *Angew. Chem., Int. Ed.* **1997**, *36*, 1011−1012.
(18) Kannarpady, G. K.; Khedir, K. R.; Ishihara, H.; Woo, J.; Oshin, O. D.; Trigwell, S.; Ryerson, C.; Biris, A. S. Controlled Growth of Self-Organized Hexagonal Arrays of Metallic Nanorods Using Template-Assisted Glancing Angle Deposition for Superhydrophobic Applications. *ACS Appl. Mater. Interfaces* **2011**, *3*, 2332−2340.
(19) Liu, H.; Szunerits, S.; Xu, W.; Boukherroub, R. Preparation of Superhydrophobic Coatings on Zinc as Effective Corrosion Barriers. *ACS Appl. Mater. Interfaces* **2009**, *1*, 1150−1153.
(20) Ebert, D.; Bhushan, B. Transparent, Superhydrophobic, and Wear-Resistant Coatings on Glass and Polymer Substrates Using SiO_2, ZnO, and ITO Nanoparticles. *Langmuir* **2012**, *28*, 11391−11399.
(21) Budunoglu, H.; Yildirim, A.; Guler, M. O.; Bayindir, M. Highly Transparent, Flexible, and Thermally Stable Superhydrophobic ORMOSIL Aerogel Thin Films. *ACS Appl. Mater. Interfaces* **2011**, *3*, 539−545.
(22) Sun, T.; Feng, L.; Gao, X.; Jiang, L. Bioinspired Surfaces with Special Wettability. *Acc. Chem. Res.* **2005**, *38*, 644−652.
(23) Bixler, G. D.; Bhushan, B. Bioinspired Micro/Nanostructured Surfaces for Oil Drag Reduction in Closed Channel Flow. *Soft Matter* **2013**, *9*, 1620−1635.
(24) Bixler, G. D.; Bhushan, B. Fluid Drag Reduction with Shark-Skin Riblet Inspired Microstructured Surfaces. *Adv. Funct. Mater.* **2013**, *23*, 4507−4528.
(25) Liu, Y.; Chen, X.; Xin, J. Can. Superhydrophobic Surfaces Repel Hot Water? *J. Mater. Chem.* **2009**, *19*, 5602−5611.
(26) Yang, J.; Zhang, Z.; Men, X.; Xu, X.; Zhu, X. A Simple Approach to Fabricate Superoleophobic Coatings. *New J. Chem.* **2011**, *35*, 576−580.
(27) Zhu, X.; Zhang, Z.; Xu, X.; Men, X.; Yang, J.; Zhou, X.; Xue, Q. Facile Fabrication of a Superamphiphobic Surface on the Copper Substrate. *J. Colloid Interface Sci.* **2012**, *367*, 443−449.
(28) Zhang, Z.; Zhu, X.; Yang, J.; Xu, X.; Men, X.; Zhou, X. Facile Fabrication of Superoleophobic Surfaces with Enhanced Corrosion Resistance and Easy Repairability. *Appl. Phys. A: Mater. Sci. Process.* **2012**, *108*, 601−606.
(29) Bae, W. G.; Song, K. Y.; Rahmawan, Y.; Chu, C. N.; Kim, D.; Chung, D. K.; Suh, K. Y. One-Step Process for Superhydrophobic Metallic Surfaces by Wire Electrical Discharge Machining. *ACS Appl. Mater. Interfaces* **2012**, *4*, 3685−3691.
(30) Barthwal, S.; Kim, Y. S.; Lim, S.-H. Mechanically Robust Superamphiphobic Aluminum Surface with Nanopore-Embedded Microtexture. *Langmuir* **2013**, *29*, 11966−11974.
(31) Zhu, Q.; Chu, Y.; Wang, Z.; Chen, N.; Lin, L.; Liu, F.; Pan, Q. Robust Superhydrophobic Polyurethane Sponge as a Highly Reusable Oil-Absorption Material. *J. Mater. Chem. A* **2013**, *1*, 5386−5393.
(32) Im, M.; Im, H.; Lee, J.-H.; Yoon, J.-B.; Choi, Y.-K. A Robust Superhydrophobic and Superoleophobic Surface with Inverse-Trapezoidal Microstructures on a Large Transparent Flexible Substrate. *Soft Matter* **2010**, *6*, 1401−1404.
(33) Su, C.; Xu, Y.; Gong, F.; Wang, F.; Li, C. The Abrasion Resistance of a Superhydrophobic Surface Comprised of Polyurethane Elastomer. *Soft Matter* **2010**, *6*, 6068−6071.
(34) Wang, H.; Xue, Y.; Ding, J.; Feng, L.; Wang, X.; Lin, T. Durable, Self-Healing Superhydrophobic and Superoleophobic Surfaces from Fluorinated-Decyl Polyhedral Oligomeric Silsesquioxane and Hydrolyzed Fluorinated Alkyl Silane. *Angew. Chem., Int. Ed.* **2011**, *50*, 11433−11436.
(35) Deng, B.; Cai, R.; Yu, Y.; Jiang, H.; Wang, C.; Li, J.; Li, L.; Yu, M.; Li, J.; Xie, L. Laundering Durability of Superhydrophobic Cotton Fabric. *Adv. Mater.* **2010**, *22*, 5473−5477.
(36) Xue, C.-H.; Ma, J.-Z. Long-lived Superhydrophobic Surfaces. *J. Mater. Chem. A* **2013**, *1*, 4146−4161.
(37) Wang, B.; Li, J.; Wang, G.; Liang, W.; Zhang, Y.; Shi, L.; Guo, Z.; Liu, W. Methodology for Robust Superhydrophobic Fabrics and Sponges from In Situ Growth of Transition Metal/Metal Oxide Nanocrystals with Thiol Modification and Their Applications in Oil/Water Separation. *ACS Appl. Mater. Interfaces* **2013**, *5*, 1827−1839.
(38) Wang, H.; Zhou, H.; Gestos, A.; Fang, J.; Lin, T. Robust, Superamphiphobic Fabric with Multiple Self-Healing Ability against Both Physical and Chemical Damages. *ACS Appl. Mater. Interfaces* **2013**, *5*, 10221−10226.
(39) Wang, C.-F.; Lin, S.-J. Robust Superhydrophobic/Superoleophilic Sponge for Effective Continuous Absorption and Expulsion of Oil Pollutants from Water. *ACS Appl. Mater. Interfaces* **2013**, *5*, 8861−8864.
(40) Peng, S.; Tian, D.; Yang, X.; Deng, W. Highly Efficient and Large-scale Fabrication of Superhydrophobic Alumina Surface with Strong Stability Based on Self-congregated Alumina Nanowires. *ACS Appl. Mater. Interfaces* **2014**, *6*, 4831−4841.
(41) Guo, Z.; Zhou, F.; Hao, J.; Liu, W. Stable Biomimetic Superhydrophobic Engineering Materials. *J. Am. Chem. Soc.* **2005**, *127*, 15670−15671.
(42) Saleema, N.; Sarkar, D.; Paynter, R.; Chen, X.-G. Superhydrophobic Aluminum Alloy Surfaces by a Novel One-Step Process. *ACS Appl. Mater. Interfaces* **2010**, *2*, 2500−2502.
(43) Zhang, Y.; Wang, H.; Yan, B.; Zhang, Y.; Yin, P.; Shen, G.; Yu, R. A Rapid and Efficient Strategy for Creating Super-hydrophobic Coatings on Various Material Substrates. *J. Mater. Chem.* **2008**, *18*, 4442−4449.
(44) Meng, H.; Wang, S.; Xi, J.; Tang, Z.; Jiang, L. Facile Means of Preparing Superamphiphobic Surfaces on Common Engineering Metals. *J. Phys. Chem. C* **2008**, *112*, 11454−11458.
(45) Feng, L.; Che, Y.; Liu, Y.; Qiang, X.; Wang, Y. Fabrication of Superhydrophobic Aluminium Alloy Surface with Excellent Corrosion Resistance by a Facile and Environment-Friendly Method. *Appl. Surf. Sci.* **2013**, *283*, 367−374.
(46) Hozumi, A.; Kim, B.; McCarthy, T. J. Hydrophobicity of Perfluoroalkyl Isocyanate Monolayers on Oxidized Aluminum Surfaces. *Langmuir* **2009**, *25*, 6834−6840.
(47) Tadanaga, K.; Katata, N.; Minami, T. Formation Process of Super-Water-Repellent Al_2O_3 Coating Films with High Transparency by the Sol−Gel Method. *J. Am. Ceram. Soc.* **1997**, *80*, 3213−3216.
(48) Fu, X.; He, X. Fabrication of Super-hydrophobic Surfaces on Aluminum Alloy Substrates. *Appl. Surf. Sci.* **2008**, *255*, 1776−1781.
(49) Liu, Y.; Yin, X. M.; Zhang, J. J.; Wang, Y. M.; Han, Z. W.; Ren, L. Q. Biomimetic Hydrophobic Surface Fabricated by Chemical Etching Method from Hierarchically Structured Magnesium Alloy Substrate. *Appl. Surf. Sci.* **2013**, *280*, 845−849.
(50) Tuteja, A.; Choi, W.; Ma, M.; Mabry, J. M.; Mazzella, S. A.; Rutledge, G. C.; McKinley, G. H.; Cohen, R. E. Designing Superoleophobic Surfaces. *Science* **2007**, *318*, 1618−1622.
(51) Cao, L.; Price, T. P.; Weiss, M.; Gao, D. Super Water- and Oil-Repellent Surfaces on Intrinsically Hydrophilic and Oleophilic Porous Silicon Films. *Langmuir* **2008**, *24*, 1640−1643.
(52) Callies, M.; Quéré, D. On Water Repellency. *Soft Matter* **2005**, *1*, 55−61.